

Article

Rare Biosphere Archaea Assimilate Acetate in Precambrian Terrestrial Subsurface at 2.2 km Depth

Maija Nuppenen-Puputti ^{1,*}, Lotta Purkamo ², Riikka Kietäväinen ³, Mari Nyysönen ¹, Merja Itävaara ¹, Lasse Ahonen ³, Ilmo Kukkonen ⁴ and Malin Bomberg ¹

¹ VTT Technical Research Centre of Finland Ltd., 02044 Espoo, Finland; mari.nyysonen@vtt.fi (M.N.); merja.itavaara@gmail.com (M.I.); malin.bomberg@vtt.fi (M.B.)

² School of Earth and Environmental Sciences, University of St Andrews, St Andrews KY16 9AL, UK; lkp5@st-andrews.ac.uk

³ Geological Survey of Finland, 02151 Espoo, Finland; riikka.kietavainen@gtk.fi (R.K.); lasse.ahonen@gtk.fi (L.A.)

⁴ Department of Physics, University of Helsinki, 00014 Helsinki, Finland; ilmo.kukkonen@helsinki.fi

* Correspondence: nuppenenpuputti@gmail.com

Received: 8 September 2018; Accepted: 8 November 2018; Published: 13 November 2018



Abstract: The deep biosphere contains a large portion of the total microbial communities on Earth, but little is known about the carbon sources that support deep life. In this study, we used Stable Isotope Probing (SIP) and high throughput amplicon sequencing to identify the acetate assimilating microbial communities at 2260 m depth in the bedrock of Outokumpu, Finland. The long-term and short-term effects of acetate on the microbial communities were assessed by DNA-targeted SIP and RNA targeted cell activation. The microbial communities reacted within hours to the amended acetate. Archaeal taxa representing the rare biosphere at 2260 m depth were identified and linked to the cycling of acetate, and were shown to have an impact on the functions and activity of the microbial communities in general through small key carbon compounds. The major archaeal lineages identified to assimilate acetate and metabolites derived from the labelled acetate were *Methanosarcina* spp., *Methanococcus* spp., *Methanlobus* spp., and unclassified *Methanosarcinaceae*. These archaea have previously been detected in the Outokumpu deep subsurface as minor groups. Nevertheless, their involvement in the assimilation of acetate and secretion of metabolites derived from acetate indicated an important role in the supporting of the whole community in the deep subsurface, where carbon sources are limited.

Keywords: deep biosphere; stable isotope probing; carbon cycling; *Methanosarcina*; *Methanococcus*; *Methanlobus*; aceticlastic methanogenesis; ICDP

1. Introduction

The deep subsurface offers a unique niche to microbial communities with challenging conditions that comprise limited carbon and energy sources, anoxia, and isolation from surface ecosystems with photosynthetically-derived carbon compounds. Deep continental crust microbial communities, however, represent a remarkable portion of the total biomass on Earth [1–3]. The importance of the deep terrestrial biosphere, its metabolic interactions with the environment, and the energy sources of the active microbial communities are still poorly understood.

In contrast to the surface biosphere, the deep subsurface biosphere carbon cycle is dependent on different anaerobic microorganisms using less energetic electron acceptors than oxygen. Kotelnikova and Pedersen [4] observed autotrophic acetogenesis in cultures from the deep granitic subsurface of Äspö, Sweden, and suggested that acetate and hydrogen could serve as possible energy sources for the deep biosphere. Further hypotheses on microbial communities possibly interacting with minerals or

utilizing soluble gases, such as crustal methane or hydrogen from radiolytic decomposition of water, have been made since [5–8]. More specifically, the metabolic capabilities of deep terrestrial subsurface microbial communities include the pathways covering, e.g., methanogenesis [9–11], anaerobic methane oxidation [12], acetogenesis [4,13], sulfate reduction [14–16], oxidation of sulfur by denitrification [17], and reduction of iron [14].

The Outokumpu deep scientific drill hole, located in Eastern Finland, hosts a unique environment piercing through crystalline Precambrian bedrock and its numerous saline fluid filled fracture zones. The composition of the microbial communities and the geochemical characteristics of the Outokumpu deep subsurface have been studied in detail [11,18–27]. The metabolic strategies of the microbial communities at different depths in Outokumpu have been estimated through functional gene analysis and metagenomes [11,21]. Purkamo et al. [21,22] suggested that microbial communities commonly employ heterotrophic carbon assimilation in the Outokumpu deep subsurface, and that the communities have the capacity of both sulphate and nitrate reduction. At greater depths, genetic potential for autotrophic acetogenesis and hydrogenotrophic methanogenesis has been detected from Outokumpu metagenomes together with H₂ oxidation and CO₂ fixation coupling hydrogenases [11].

The terrestrial deep subsurface represents an oligotrophic, nutrient-poor, and isolated habitat. The fact that heterotrophy appears to be common in the Outokumpu deep biosphere means that the carbon substrates for the heterotrophic microorganisms must either be derived from ancient carbon compounds embedded in the rock, or synthesized by autotrophic microorganisms. The reductive acetyl-CoA-pathway was recognized as a key carbon fixation route at a depth of 3.3 km in the Tau Tona gold mine in South Africa [28]. This pathway is linked both to the formation of methane by archaea and to the formation of acetate by bacteria [13,29]. Acetate is a possible key-intermediate substrate in the deep biosphere [13,30–32]. In addition to production by acetogenic microbial communities, acetate could be formed in the deep biosphere by the decomposition of organic matter. Abiotic formation of acetate at high pH and high hydrogen conditions has also been suggested [33]. Deep subsurface acetogenic microbes may support further groups, such as acetate-oxidizing sulfate reducing bacteria [21,31] or acetate utilizing methanogens [32]. In the Outokumpu subsurface sulfate reducers have been detected at various depths [21], and enrichment of acetate-consuming microbial communities from the depth of 967 m was observed with acetate amended microcosms [30].

The great majority of deep biosphere microorganisms remain uncultivable in laboratory conditions, setting limits to research on their energy and carbon sources. Stable isotope probing (SIP), first introduced by Radajewski et al. [34], is an advantageous method in the analysis of metabolism routes in the environment and characterization of species linked to assimilation of the studied substrate [35]. SIP has been successfully used on a broad scale in environmental microbiology, revealing the species linked to actively performed functions [36–39].

Acetate can support methanogens, and thus, the compounds formed can activate further microbial groups. We aimed to identify and characterize active acetate-utilizing communities in the Outokumpu deep subsurface fracture fluids by DNA SIP and cell activation. We compared the community response to acetate in two different timescales, rapid response to the given substrate by analyzing the community RNA after a short incubation period (hours), and long term community response by analyzing the community DNA 2.5 weeks after incubation. We aimed to optimize and evaluate the suitability of SIP for studying deep subsurface microbial communities, which generally present low cell numbers and possibly slow metabolism rates of the microorganisms in their austere environment.

2. Materials and Methods

2.1. Site Description

The Outokumpu Deep Scientific Drill Hole is part of the International Continental Scientific Drilling Program (<https://www.icdp-online.org/projects/world/europe/outokumpu-finland/>) research infrastructure. The Outokumpu deep drill hole, located in eastern Finland (62.71740° N,

29.06528° E), was drilled in 2006 and has previously been described in [11,18–27]. Briefly, the fracture zone at 2260 m contain saline water, with methane as dominating dissolved gas and an in situ temperature around 37 °C (Table 1). The geochemistry of the sampling site in June 2010 has been described by Kietäväinen et al. [25] and water chemistry at the depth of 2260 m by Purkamo et al. [20]. The number of microbial cells at the time of sampling was 1.5×10^3 cells/mL (Table 1).

Table 1. Hydrogeochemical characteristics of water and gas samples, and fluid cell count values in Outokumpu subsurface at the depth of 2260 m.

Measurement	Value	Reference
Temperature, °C	37.1 °C	[20]
pH	9.3	[40]
Alkalinity (mM)	0.25	[20]
EC (mS cm^{-1} 25 °C)	47.5	[20]
SO ₄ (mg/L)	<10	[25]
Sulphide (mg/L)	0.42	[25]
S (mg/L)	4.81	[20]
TDS (g/L)	31	[40]
TOC (mg/L)	27.2	[40]
DOC (mg/L)	22.5	[40]
DIC (mmol/L)	0.21	[26]
Ar (vol%)	0.23	[26]
CO ₂ (vol%)	b.d.	[26]
CH ₄ (vol%)	77	[26]
N ₂ (vol%)	17	[26]
H ₂ (vol%)	0.17	[26]
He (vol%)	2.8	[26]
C ₂ H ₆ (vol%)	0.39	[26]
C ₃ H ₈ (vol%)	0.012	[26]
Prevalent rock type	Biotite gneiss	[22,41]
Cell count (cells/mL)	1.5×10^3	[20]
Bacterial 16S rRNA gene copy number/mL	9.01×10^2 (SEM 3.72×10)	[20]
Archaeal 16S rRNA gene copy number/mL	2.32×10 (SEM 1.07)	[20]
<i>dsrB</i> gene copy number (copies/mL)	1.7×10^2	[20]

b.d.: below detection limit; SEM: standard error of mean.

2.2. Sampling

Sample fluid was collected in June 2010 by pumping through a poly amide (PA) tube, as described previously [20,23,25]. The drill hole was sealed with one air-inflated packer situated at the depth of 1190 m. The use of only one packer instead of two flanking the actual fracture zone was due to a narrowing of the drill hole at 1190 m depth due to movement of the rock. Thus, only one packer could be used. The PA tube was unused and factory clean and filled with filter-sterilized reverse osmosis (RO) water before it descended into the drill hole to the depth of 2260 m. In order to collect fracture fluid, water was pumped from the drill hole from the 2260 m depth continuously for 2.5 weeks. Sample fluid was lead via an air-tight sterilized PA tube into a portable anaerobic glove box (GB-2202-2, MBRAUN, Garching, Germany) where sample fluid was collected under N₂ (99.999%) flow. Anaerobic conditions were further enhanced with anaerobic generators (Anaerocult A, Merck, Darmstadt, Germany). Average fluid flow-rate was 2–5 L·h⁻¹. Fluid was first collected in a 2 L acid washed sterile Schott Duran bottle (Duran Group, Wertheim/Main, Germany) prior to further handling. In order to obtain sufficient amounts of biomass, the microbial cells in the water samples were first concentrated on filters. Furthermore, to enhance labelling of nucleic acids of active acetate utilizers, double-labelled 99% ¹³C-acetate was used. DNA-based SIP was used to evaluate the carbon flow in the microbial communities, and RNA-based cell activation was applied to address the primary activation linked to the acetate amendment.

Microbial cells from 10 L and 1 L samples of fluid were collected on Millipore 0.2 μm polyethersulfone-membrane (PES) (Corning, Tewksbury, MA, USA) for DNA and RNA analyses, respectively. For long-term incubations, the filters were cut out of the filter funnels and placed into headspace bottles amended 75 mL of the fracture zone fluid combined with acetate treatment. The bottles were sealed with gas tight butyl rubber stoppers and aluminium crimp caps and stored at +4 °C in a cool-box for transport to the laboratory incubation. The short-term incubations were performed directly on the filter units in the anaerobic glove box immediately after collection and concentration of the biomass samples.

The microcosms and filter incubations were amended with ^{13}C -acetate or ^{12}C -acetate suspended in fracture fluid to a final concentration of 4 mM. The long-term incubations received 75 mL and the short-term ones 50 mL of the acetate amended fracture fluid suspension. Altogether, six replicate long-term and short-term incubations were prepared, of which triplicate treatments were with ^{13}C -acetate and with ^{12}C -acetate, respectively. The long-term incubations were kept at 30 °C for 2.5 weeks, protected from light. At the end of the incubation, the microbial biomass was collected on 0.2 μm cellulose-acetate (CA) filter membranes (Millipore). The CA filter was cut out from the funnel and stored separately from the PES filter. Both the incubated PES filter and the CA filter from the end of the experiment were transferred to a 50 mL centrifuge tube and kept frozen at -80 °C until further analysis. The short-term incubations performed directly on the filter units were kept in the anaerobic glove box together with the substrate for 3 h after which the liquid was removed from the filter units by filtration, and the filter containing the concentrated biomass was removed from the funnel with a sterile scalpel and stored in a 50 mL plastic test tube in dry ice for transport to the laboratory, and stored at -80 °C until further analysis.

In addition, one 10 L control sample for the DNA profile and two 1 L samples for the RNA profile of the microbial community at the time of sampling were collected, filtered on PES membrane, and stored as described above.

2.3. Nucleic Acid Extraction

DNA was extracted from the original fracture fluid and long-term incubated microcosm samples with the Metagenomic DNA Isolation Kit (EPICENTRE Biotechnologies, Madison, WI, USA) according to the manufacturer's instructions. The filters were cut into small slices with a sterile scalpel before they were subjected to the extraction protocol. The extracted DNA from the CA (end of incubation) and PES (incubated filter) was eluted in 50 μL and 100 μL TE buffer, respectively. The DNA sample for further handlings was combined from both PES and CA extractions. The extracted DNA was stored at -80 °C. RNA was extracted from the PES filters with the PowerWater RNA isolation Kit (MoBio Laboratories Inc., Carlsbad, CA, USA) according to the manufacturer's instructions. The filters were placed into the PowerWater Bead tube as such. The RNA concentration was analysed with the NanoDrop ND-1000 UV-Vis Spectrophotometer (NanoDrop Technologies Inc., Wilmington, DE, USA). The extracted RNA was stored at -80 °C.

2.4. Ultracentrifugation and Gradient Fractionation

The ultracentrifugation was performed to separate the labelled ^{13}C -containing nucleic acids from total nucleic acids. DNA samples and reagents were prepared, and ultracentrifugation was performed using a gradient fractionation protocol according to Neufeld et al. [42]. The maximum yield of sample DNA (0.2–2.8 μg DNA for ^{12}C samples and 0.5–2.3 μg DNA for ^{13}C samples) was mixed with gradient buffer (0.1 M Tris, 0.1 M KCl, 1 mM EDTA). A total of 708 μL of DNA/gradient buffer-solution was further mixed with 4.9 mL of CsCl-stock solution, loaded into Beckmann 5.1 mL ultracentrifuge polypropylene tubes (BeckmannCoulter, Brea, CA, USA), and sealed with a heat sealer tube topper (Beckmann Coulter, Inc., Brea, CA, USA). The final density of the mixed solution before the centrifugation was $1.722\text{ g}\cdot\text{mL}^{-1}$. Control tubes without nucleic acids (blank controls) were included in each centrifugation to evaluate the formation of the gradient.

The samples were centrifuged with a Beckmann ultracentrifuge VTI 65.2 rotor for 60 h at 20 °C, with maximum acceleration and no deceleration with 44,100 rpm for DNA and samples. The formed gradient was fractionated from the tubes immediately after centrifugation in a laminar flow hood. The ultracentrifuge tubes were pierced at the bottom and from the top with a 23-gauge 1" needle. The gradient solution was replaced by dyed DEPC-treated water, injected to the tube from the top using a syringe pump (New Era Pump Systems, Inc., Farmingdale, NY, USA) with a 200 $\mu\text{L}\cdot\text{min}^{-1}$ flow rate. Fractions were collected from the bottom of the ultracentrifuge tubes into 2 mL Eppendorf tubes. DNA fractions were collected in 50 s intervals resulting in total of 22 fractions for each DNA sample. The density of each fraction in the control tube was measured with a refractometer (DR301-95, A. Krüss Optitronic, Hamburg, Germany) to verify the formation of the gradient. The formation of a gradient in the sample-bearing tubes was confirmed by measuring the density of the first and last fraction from each ultracentrifugation tube.

2.5. Desalting of the Fractions

Nucleic acids were precipitated from the fractions by adding 2 volumes of isopropanol followed by an incubation of samples at $-20\text{ }^{\circ}\text{C}$ for a minimum of one day. The precipitated nucleic acids were pelleted by centrifugation for 20 min at 14,000 G at $4\text{ }^{\circ}\text{C}$ in a table top centrifuge (Eppendorf, Hamburg, Germany). The supernatant was discarded, avoiding the pellet, and 150 μL of isopropanol was added. Samples were centrifuged 5 min at 16,000 G at $4\text{ }^{\circ}\text{C}$. The isopropanol was carefully removed and the nucleic acid pellet was rinsed with ice cold 70% ethanol to remove the remaining salts. In order to purge any residual ethanol, the samples were centrifuged for 5 min at 16,000 G at $4\text{ }^{\circ}\text{C}$, the remaining supernatant was discarded, and the nucleic acid pellets were briefly air dried under a laminar flow. The DNA pellets were re-suspended in 30 μL of Tris-EDTA buffer (TE). The desalted nucleic acids were kept frozen at $-20\text{ }^{\circ}\text{C}$ until further analysis.

2.6. Identification of Heavy Nucleic Acid Fractions

Quantitative PCR (qPCR) was applied in order to identify the location of the ^{13}C labeled heavy nucleic acid fractions by estimating the relative abundances of bacterial 16S rRNA gene copies in the fractions of each sample. White 96-well FrameStar[®] plates (4titude, Surrey, UK) were used for the qPCR amplifications performed on a Roche LightCycler LC480 (Roche, Penzberg, Germany).

The qPCR was performed with a KAPA[™] SYBR[®] FAST qPCR Master Mix (2 \times) Light cycler 480 Kit (Kapa Biosystems, Wilmington, MA, USA) with triplicate reactions for each DNA fraction. The amplification was performed with the primers fD1 [43] and P2 [44] (Table 2) amplifying fragment between nucleotide sites 8 and 534 (*E. coli* numbering) of the bacterial 16S rRNA gene. The reaction volume was 10 μL , containing 5 μL of 2 \times KAPA master mix, 0.15 μL of each primer (100 μM stock) and 3.3 μL molecular grade water (Sigma, Saint Louis, MO, USA) and 1 μL of DNA template. The qPCR programme consisted of an initial denaturation at $95\text{ }^{\circ}\text{C}$ for 15 min, 35 cycles of 10 s at $95\text{ }^{\circ}\text{C}$, 35 s at $54\text{ }^{\circ}\text{C}$, and 30 s at $72\text{ }^{\circ}\text{C}$, and a final elongation step for 3 min at $72\text{ }^{\circ}\text{C}$. The qPCR programme ended with melting curves analysis of 10 s at $95\text{ }^{\circ}\text{C}$, 1 min at $65\text{ }^{\circ}\text{C}$, and continuous melting at $95\text{ }^{\circ}\text{C}$.

Table 2. Primers used in this research.

Primer	In This Research	Target	Reference
fD1	qPCR	Bacterial 16S rRNA	[43]
P2	qPCR, amplicon library PCR	Bacterial 16S rRNA	[44]
8F	Amplicon library PCR	Bacterial 16S rRNA	[45]
A109F	Initial PCR for Archaea	Archaeal 16S rRNA	[46]
Arch915R	Initial PCR for Archaea	Archaeal 16S rRNA	[47]
A344 ¹	Nested amplicon library PCR	Archaeal 16S rRNA	[48]
A744 ¹	Nested amplicon library PCR	Archaeal 16S rRNA	[49]

¹ Tag-pcr primers with an attached adapter and barcode sequences at 5' end of the primer.

qPCR data was analyzed with the Light Cycler[®] 1.5 SW program 1.5.0 (Roche Applied Science, Mannheim, Germany). Location of heavy nucleic acid fractions was identified by comparing CsCl-densities and ratio of gene copies to maximum quantity of detected nucleic acids in ¹²C and ¹³C samples (percentage of total amounts).

2.7. Reverse Transcription

The RNA from the total enriched community and original fracture fluid was converted to cDNA using Superscript III reverse transcriptase kit (Invitrogen, Life Technologies, Ltd., Carlsbad, CA, USA) and random hexamers. The reaction mixture was made with 0.5 µL of random primers of 0.5 µg·µL⁻¹ stock (Promega, Madison, CA, USA), 1 µL dNTP of 10mM stock (Promega), 11 µL of the RNA template, and molecular-grade-water to a total reaction volume of 20 µL. The samples were heated to 65 °C for 5 min and chilled to 4 °C for 1 min. Hereafter, 4 µL of the reaction buffer, 1 µL DTT (Invitrogen, Carlsbad, CA, USA), 1 µL RNase inhibitor of 40 U·µL⁻¹ stock (Promega), and 1 µL of Superscript III reverse transcriptase of stock 200 U·µL⁻¹ (Invitrogen, Carlsbad, CA, USA) was added to the reaction. The reactions were mixed by pipetting and then incubated at 25 °C for 5 min and heated for 50 °C for 50 min. The reaction was inactivated by heating to 85 °C for 5 min, and ended by chilling to 4 °C.

2.8. Whole Genome Amplification

Identified heavy nucleic acid fractions were combined to a separate representative sample for each microcosm for whole genome amplification (WGA). The WGA reaction was performed in duplicates for all DNA and cDNA samples with the Illustra GenomiPhi V2 DNA Amplification kit (GE Healthcare, Piscataway, NJ, USA) according to the manufacturer's instructions. A mixture of 2 µL of template and 18 µL of sample buffer was first heated to 95 °C for 3 min. The reactions were then cooled on ice and 18 µL of reaction buffer and 2 µL of enzyme-mix were added to each reaction while kept on ice followed by incubation at 30 °C for 2 h and a post-amplification at 65 °C for 10 min before a final cooling to 4 °C.

2.9. Amplicon Library Preparation

The archaeal 16S rRNA genes were amplified using a nested PCR approach. In the first round PCR, the archaeal 16S rRNA genes were amplified primers with A109F and 915R amplifying a 806 bp fragment of the archaeal 16S rRNA gene (Table S1). The first round PCR product was used as template for the second round (nested PCR) for the amplicon libraries, which was performed with primers A344f and A744r [48,49] (Table 2). The preparation of the barcoded bacterial 16S rRNA gene amplicons was carried out by single round PCR using primers 8f and P2 covering the V1–V3 regions of the bacterial 16S rRNA gene (Table 2). The primers used for the amplicon libraries were equipped with adapters for the 454 FLX platform, and each forward primer contained unique 6-nucleotide long barcode sequence as described by Bomberg et al. [50]. The archaeal and bacterial amplicon library PCR was performed as described in Table S1. All performed PCR runs included negative control samples. The PCR programme consisted of initial denaturation at 98 °C for 30 s followed by 40 cycles of 10 s at 98 °C, 15 s annealing at 50 °C for archaea and 55 °C for bacteria, 30 s at 72 °C, and a terminal elongation step 5 min at 72 °C. All PCRs were performed with an Eppendorf Mastercycler gradient (Eppendorf, Hamburg, Germany). The amplification success, size of the amplicons, and performance of the control samples was checked with gel electrophoresis.

2.10. Sequencing and Sequence Analysis

Archaeal and bacterial 16S rRNA gene-barcoded amplicons were sequenced with the 454 Roche FLX Titanium pyrosequencing platform at the Institute of Biotechnology (University of Helsinki, Finland). The amplicon sequence data was edited and analyzed with the Mothur programme [51]. Sequences were trimmed by removing the adapter and barcode, and screened with set values for the maximum differences in primer sequence (2 nucleotides) and maximum homopolymer stretches

(8 nucleotides). The sequences were aligned against the SILVA-reference alignment Silva.seed v_123 [52] and alignments were screened to match defined start- and end-positions with the minimum sequence length of 160 bp for bacteria and 140 bp for archaea. The chimeric sequences were identified with Mothur's chimera slayer command and removed from the data. The clustering of sequences into OTUs was done with the nearest neighbor parameter based on 97% sequence homology within the OTU. Bacterial and archaeal OTUs were classified using Silva reference taxonomy (v_132) [52]. OTUs that did not receive any classification were removed from the bacterial data. Mothur was used to determine the representative sequences for the OTUs, analyze the relative abundance of OTUs and sequences, and to generate biom-files. Part of the unclassified OTU sequences were checked with BLAST-tool against the NCBI database (<https://blast.ncbi.nlm.nih.gov/Blast.cgi>) [53].

2.11. Statistical analysis

The microbial community data were further analysed in RStudio with imported biom-file constructed in Mothur [54]. OTUs containing only single sequences were removed, after which the data was normalized with the MetagenomeSeq package's cumulative sum scaling (CSS) normalization in R [55]. Principal coordinate analysis (PCoA) in R's Phyloseq package [56] was used to estimate the dissimilarities between the active microbial communities (SIP) and total microbial communities, and again between DNA and RNA communities. The PCoA was built with Bray-Curtis distance model and the calculation of the eigenvalues used 999 random repeats in R's vegan package [57]. Alphadiversity measurements, including the detected number of sequences, Chao1 richness estimate, and Shannon's and Simpson's diversity indices, were calculated from raw data and normalized (rarefied) data with R's vegan package. Sequence data was rarefied to 136 and 150 sequences in archaeal and bacterial data, respectively.

2.12. Accession Numbers

Sequences obtained in this study are deposited in the European nucleotide Archive (ENA) under project PRJEB28401.

3. Results

3.1. Identification of Heavy Fractions

DNA samples were distributed to 22 fractions (Figure S1). The location of DNA in the CsCl gradient was estimated by comparison of relative abundances of bacterial 16S rRNA gene copies in different fractions. The labelled ^{13}C DNA was located at CsCl densities $1.732\text{--}1.728\text{ g}\cdot\text{mL}^{-1}$, from which the labeled DNA was pooled from four fractions to one sample (Figure S1 and Table 3). The location of unlabeled environmental DNA of the ^{12}C amended samples was detected at densities lighter than $1.716\text{ g}\cdot\text{mL}^{-1}$. In addition, unlabeled DNA could be observed in both ^{13}C and ^{12}C amended samples at densities lighter than $1.640\text{ g}\cdot\text{mL}^{-1}$.

Table 3. The description of the terms and sample names used in text or figures.

Term	Sample Names	Sample Volume (L)	Incubation Time	Description
Original sample	DNA_0	10	0	Original sample that represents the microbial communities in the drill hole fracture fluids at 2260 m depth at the time of the sampling
	RNA_0	1	0	
Enriched microcosms	DNA_E1, DNA_E2, DNA_E3	10	2.5 weeks	Samples from the microcosms incubated with acetate. Samples were not fractionated prior to analysis and thus describe changes in total microbial community in comparison to the original sample.
	RNA_E1, RNA_E2, RNA_E3	1	3 h	
Labelled fraction	DNA_F1, DNA_F2, DNA_F3	10	2.5 weeks	Samples that represents the ^{13}C -labelled fraction of the microbial communities carrying heavy isotopes in their DNA

3.2. Alphadiversity Measures

The Shannon diversity indices (H') of the archaeal communities of the original and enriched samples varied in rarefaction normalized data from 0.1 to 1.1 (with the exception of sample RNA-E2 that had $H' = 2.2$) both from DNA and RNA (Table 4). Only two distinct archaeal OTUs were detected

in the original samples. In contrast, the archaea detected from the labelled fractions had high Shannon index values, varying from 1.3–3.3, indicating higher diversity. The Simpson diversity indices showed similar result for the archaeal communities, i.e., the OTU richness was higher in the ^{13}C labelled fractions. The Chao1 richness estimator predicted an even higher number of OTUs, especially in the heavy fractions with values 6–48 for DNA samples, respectively.

Table 4. Alphadiversity analysis of the archaeal community detected from the DNA and RNA of the original fracture fluid (DNA_0 and RNA_0, respectively), enriched microcosms (DNA_E1-3 and RNA E1-3) and the acetate assimilating community detected from the labelled fractions (DNA-F1-3). This table presents both the number of sequences (No of Seqs) and OTUs (No of OTUs) along with Chao1 richness estimate and Shannon and Simpson diversity indices, respectively, and shows both raw data and normalized (rarefied) data based calculations.

Sample ID	No Seqs	No OTUs	Chao1 Rarefied	Chao1 Raw	Shannon Rarefied	Shannon Raw	Simpson Rarefied	Simpson Raw
DNA_0	299	2	2	3	0.1	0.2	0.1	0.2
DNA_E1	597	2	2	2	0.2	0.2	0.1	0.4
DNA_E2	426	2	2	2	0.4	0.4	0.2	1.1
DNA_E3	138	3	6	6	1.1	1.1	0.6	0.2
DNA_F1	1336	77	44	70	3.3	3.6	1.0	3.6
DNA_F2	1818	62	48	60	2.3	2.7	0.8	2.7
DNA_F3	2419	10	6	7	1.3	1.3	0.6	1.3
RNA_0	454	2	2	2	0.4	0.4	0.3	0.4
RNA_E1	12676	4	2	4	0.1	0.2	0.1	0.2
RNA_E2	4474	66	61	66	2.2	2.6	0.8	2.6
RNA_E3	2529	2	2	3	0.6	0.6	0.4	0.6

The Shannon indices for the bacterial communities of the rarefied original samples were 2.5 and 2.6 for DNA and RNA samples, respectively (Table 5). The highest number of OTUs was identified in the original samples, with 80 and 67 OTUs from DNA and RNA, respectively. The enriched samples showed variability in the Shannon indices varying from 0.8 to 3 in raw data, and 2.1 to 2.8 in the normalized data. Normalization by rarefaction excluded the samples DNA_E2 and DNA_E3 with lowest sequence counts. Simpson diversity indices, however, demonstrated lower variability in diversity in the bacterial communities (values 0.6–0.9 in raw data and 0.7–0.9 in rarefied data, respectively). Chao1 OTU richness estimator demonstrated the highest values in rarefied original samples with 80 and 58 estimated OTUs for DNA and RNA, respectively.

Table 5. Alphadiversity analysis of the bacterial community detected from the DNA and RNA of the original fracture fluid (DNA_0 and RNA_0, respectively), enriched microcosms (DNA_E1-3 and RNA E1-3) and the acetate assimilating community detected from the labelled fractions (DNA-F1-3). This table presents both the number of sequences (No of Seqs) and OTUs (No of OTUs) along with Chao1 richness estimate and Shannon and Simpson diversity indices, respectively, and shows both raw data and normalized (rarefied) data based calculations.

Sample ID	No Seqs	No OTUs	Chao1 Rarefied	Chao1 Raw	Shannon Rarefied	Shannon Raw	Simpson Rarefied	Simpson Raw
DNA_0	4534	80	80	151	2.5	2.8	0.9	0.9
DNA_E1	3502	68	23	137	2.8	3	0.9	0.9
DNA_E2	13	5	-	7	-	1.7	-	0.8
DNA_E3	60	5	-	11	-	0.8	-	0.4
DNA_F1	211	22	32	29	2.5	2.8	0.9	0.9
DNA_F2	187	16	7	23	2.4	2.3	0.9	0.9
DNA_F3	3262	9	40	14	1.5	1.5	0.7	0.7
RNA_0	2953	67	58	135	2.6	2.8	0.8	0.9
RNA_E1	166	25	41	57	2.7	2.8	0.9	0.9
RNA_E2	376	27	30	44	2.1	2.3	0.7	0.8
RNA_E3	564	33	52	41	2.2	2.4	0.8	0.8

3.3. Principal Coordinates Analysis (PCoA)

In the PCoA analysis, the archaeal communities in the original fracture fluid detected by both DNA and RNA (DNA-0 and RNA-0) clustered closely together indicating high similarity between the total (DNA) and active (RNA) communities (Figure 1, Table 3). In addition, the close clustering of most of the DNA-derived heavy fractions and enriched RNA samples indicated that the main users of acetate after 2.5 weeks of incubation were also the taxa that responded rapidly to the added acetate, with only one heavy fraction DNA sample separating slightly from the rest of the ^{13}C labelled fractions. The enriched RNA microcosm samples had the most variation within their sample type and compared to the original and labelled samples.

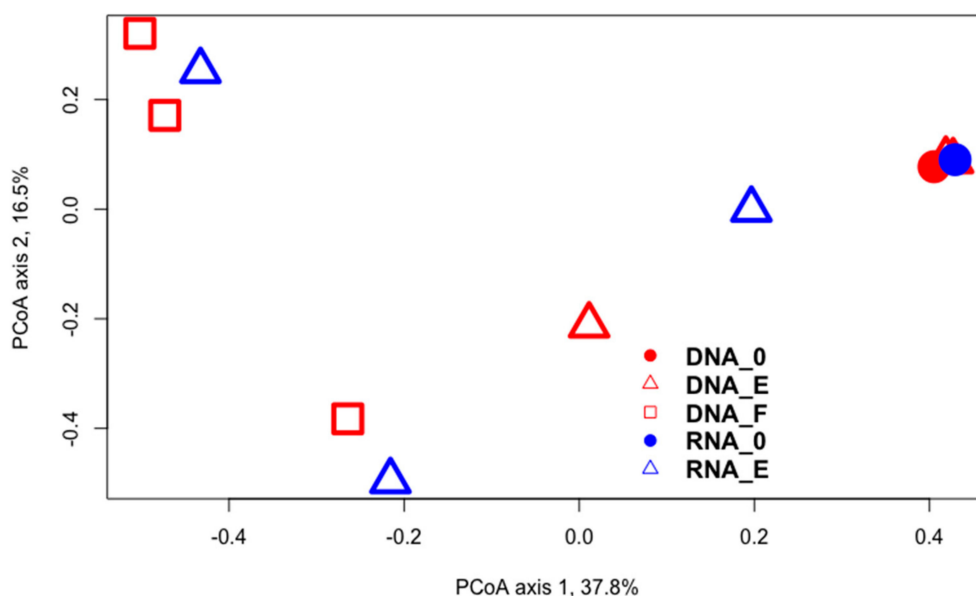


Figure 1. PCoA plot on archaeal samples. Samples DNA_0 and RNA_0 are the samples representing original fracture fluids. Samples DNA_E and RNA_E are enriched microcosm samples and DNA_F represent acetate assimilating labelled fractions. Axis 1 and 2 explain 37.8% and 16.5% of the variance, respectively.

In the bacterial data, the original and enriched samples grouped together, although the labelled samples scattered as two separate subgroups (Figure 2, Table 3). The bacterial communities detected from the DNA and RNA had high dissimilarities and formed separate groups according to the sample type. Nevertheless, the PCoA analysis on both the archaeal and bacterial communities demonstrated that the separation of ^{13}C -labelled fractions from the whole community of the enriched samples was successful. Thus, the acetate assimilating communities could be distinguished from the original fracture fluid community and the communities that were enriched in the microcosms.

3.4. Taxonomy

3.4.1. Archaea

The main archaeal groups in the original sample and enriched samples belonged to the family *Methanobacteriaceae* with species affiliating with the genus *Methanobacterium* (Figure 3, Table 3). The labelled DNA fractions representing the acetate consuming archaeal community hosted OTUs affiliating with the families *Methanosarcinaceae* (0.0–99.6%) and *Methanococcaceae* (0.4–99.9%). Further, the detected genera within these families were *Methanococcus* spp., *Methanolobus* spp., *Methanosarcina* spp., and a high number of OTUs affiliating with a genus of unclassified *Methanosarcinaceae* (Figure 3). OTUs in the original RNA sample represented only *Methanobacterium* spp. (100%) (Figure 3). Furthermore, low numbers of sequences belonging to genus *Archaeoglobus* spp.

were detected in two labelled fractions (DNA). Additionally, two enriched samples, DNA-E3 (66.7%) and RNA-E1 (100%), hosted *Halobacteriales* sequences. DNA sample hosted OTUs affiliating with both genus *Haloparvum* spp. and unclassified *Haloferaceae*, while RNA sample hosted OTUs affiliating with genus *Halobacterium* spp.

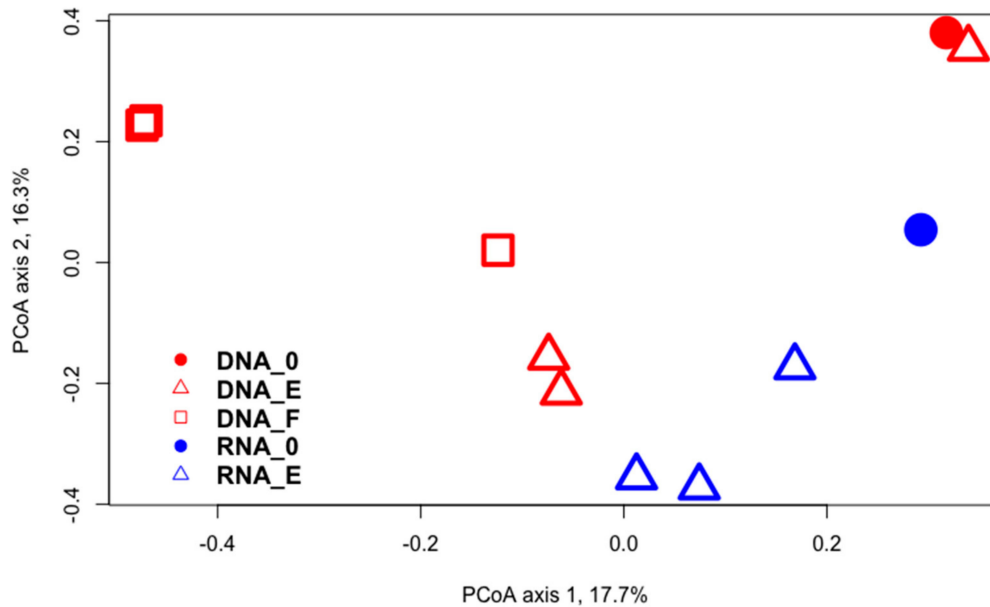


Figure 2. PCoA plot on bacterial samples. Samples DNA_0 and RNA_0 are the samples representing original fracture fluids. Samples DNA_E and RNA_E are enriched microcosm samples and DNA_F represent acetate assimilating labelled fractions. Axis 1 and 2 explains 17.7% and 16.3% of the variance, respectively.

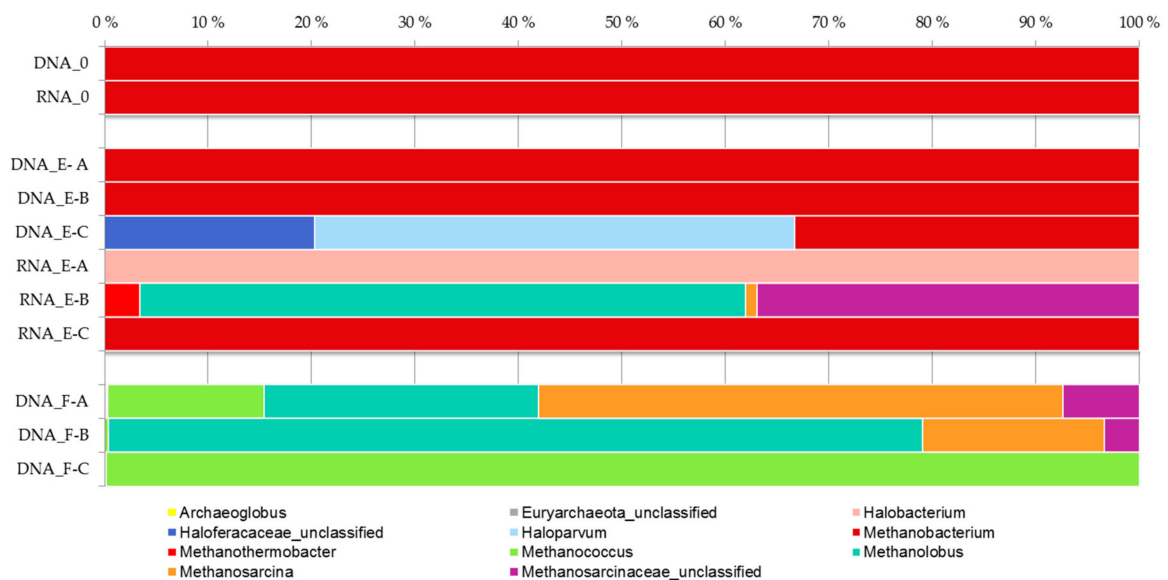


Figure 3. Taxonomy of archaeal 16S rRNA gene OTUs. Samples representing the original fracture fluid: DNA_0 and RNA_0, enriched samples representing the communities in the incubated microcosms DNA_E—samples A, B, C (DNA) and RNA_E—samples A, B, C (RNA) and the labelled fractions: DNA_F—samples A, B, C (DNA-SIP); X-axis visualizes the detected genera (percentage of total number of sequences detected) and Y-axis illustrates the sample types.

3.4.2. Bacteria

The major bacterial phyla in the original fracture fluid detected from the DNA were *Proteobacteria* and *Actinobacteria* (Figure 4, Table 3). The major genus on the actinobacterial phylum was OPB41 representing 48.1% of the sequences in the original DNA sample (Table S3). The main identified proteobacterial families in the original samples belonged to *Burkholderiaceae*, while 20% of all proteobacterial sequences belonged to unclassified *Betaproteobacteriales*. Of the sequences falling within *Burkholderiaceae*, more than 95% belonged to thus far unclassified members of the *Burkholderiaceae*. Approximately 1% of the bacteria detected from the original DNA sample affiliated with the genus *Pseudomonas*, 5% affiliated with unclassified Bacteria, and for 1% of the sequences, the domain could not be determined. The majority of the bacterial OTUs present in the labelled DNA fractions belonged to the proteobacterial phylum, more specifically, to the families *Burkholderiaceae* and *Pseudomonadaceae* (Figure 4, Table S3). The majority of the OTUs from the labeled DNA affiliated with the family *Burkholderiaceae*, and taxonomically divided further into the genera *Comamonas* spp., *Duganella* spp. and *Janthinobacterium* spp., together with unclassified *Burkholderiaceae* (Figure 5, Table S4).

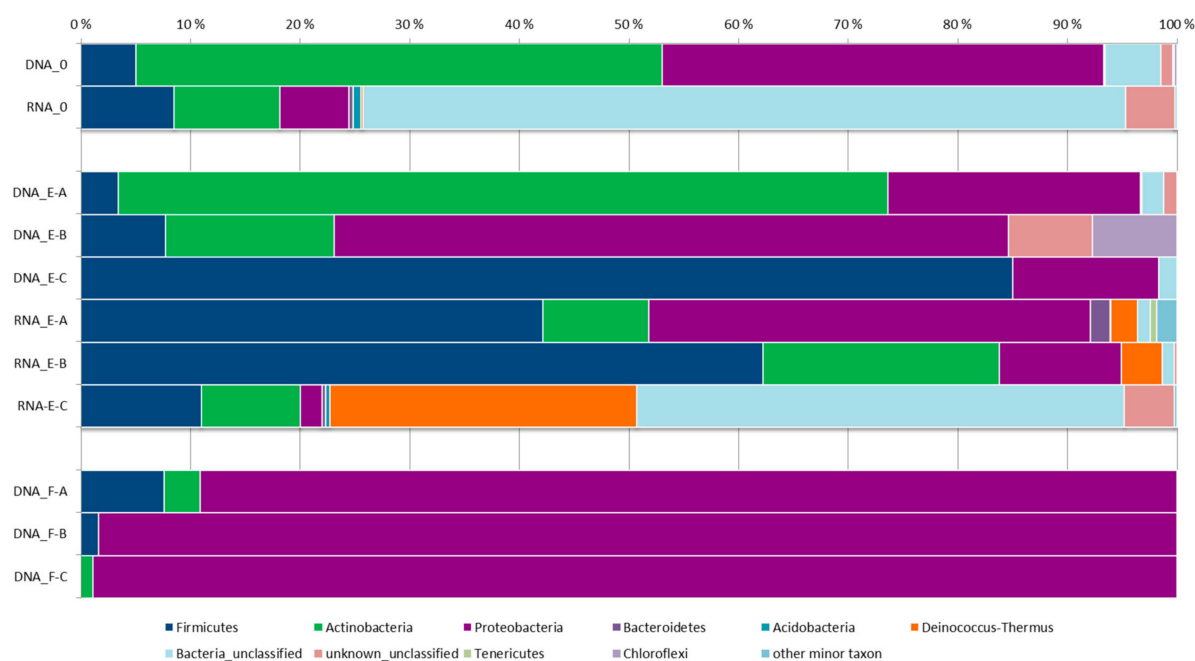


Figure 4. Taxonomy of bacterial 16S rRNA gene OTU sequences at phylum level. First are the samples representing the original fracture fluid: DNA_0 and RNA_0 followed by the enriched samples representing the communities in the incubated microcosms: DNA_E—samples A, B, C (DNA) and RNA_E—samples A, B, C (RNA). At the bottom are the labelled DNA_F—samples A, B, C (DNA-SIP). The used cut-off value for this illustration was ≥ 6 sequences/OTU/sample.

The majority of the bacteria (70%) detected from the RNA from the original fracture fluid communities affiliated with unclassified Bacteria (Figure 4). The major identified bacterial families in the original RNA samples belonged to the phylum Proteobacteria, Firmicutes, and Actinobacteria, with the majority affiliating with families OPB41 (6%), D8A-2 (3%), and *Burkholderiaceae* (2.3%) (Figure 4). The major groups in Proteobacteria included unclassified *Burkholderiaceae*, hosting 37%, and unclassified *Acetobacteraceae* (25% of the proteobacterial sequences). For nearly 5% of the remaining sequences, the domain could not be determined. All short-term enriched samples (RNA_E) hosted OTUs affiliating with *Deinococcaceae*, which were not detected in the RNA from the original sample. Furthermore, *Pseudomonas* spp. affiliating OTU-sequences had higher relative abundance at the genus level in the labelled samples from DNA SIP compared to original ground water samples. The original and enriched RNA samples hosted mainly unclassified Bacteria, with OTU sequences

closest BLAST matches to e.g., halophilic sulfate reducers *Desulfotomaculum halophilum* [58] and other uncultured *Clostridiales*. Bacterial RNA data hosted sequences that are clearly deriving from the human contamination e.g., *Streptococcaceae* (Table S4) or have been detected as contaminants in molecular biology kits, such as *Sphingomonas* spp. [59,60]. Amplicon PCR controls were negative on all PCR runs.

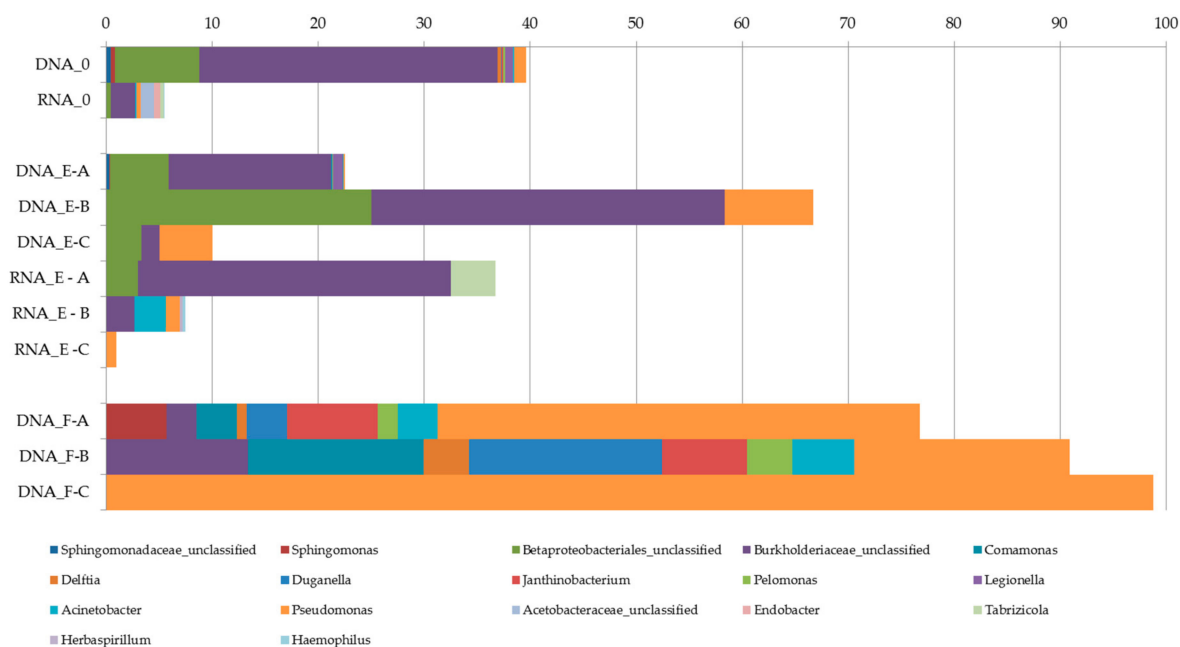


Figure 5. *Burkholderiaceae* and *Pseudomonadaceae* OTU taxonomy at genus level based on bacterial 16S rRNA gene. First are the samples representing the original fracture fluid: DNA_0 and RNA_0 followed by the enriched samples representing the communities in the incubated microcosms: DNA_E—samples A, B, C (DNA) and RNA_E—samples A, B, C (RNA). At the bottom are the labelled DNA_F—samples A, B, C (DNA-SIP). The used cut-off value for this illustration was ≥ 6 sequences/ OTU/sample.

4. Discussion

The Fennoscandian deep biosphere contains highly diverse microbial communities with rather low cell counts [20,50,61–63]. Although the community compositions have been extensively studied and found to contain a multitude of metabolic potential, only few studies exist to date that show the utilization of specific carbon sources by the deep subsurface community. To our best knowledge, no data has been published that identifies acetate utilizers from such a great depth as 2260 m. Kotelnikova and Pedersen [32] detected methanogenesis in cultivation experiments amended with acetate, methanol, or TMA in samples from the depth of 414 m in Äspö. However, the shallower site at 68 m depth presented the fastest rate for acetate-utilizing methanogenesis. Recently, Purkamo et al. [30] showed that specific bacteria were enriched in cultures containing acetate as a carbon source at 967 m depth in Outokumpu, but verification of which microbial taxa that assimilate acetate at great depth has not been reported before. In this study, we designed a SIP method for the identification of rapid activation and assimilation of acetate as well as for long-term assimilation of acetate by low cell number microbial communities retrieved from 2.2 km depth in Outokumpu. Previously undetected taxonomic groups were identified from Outokumpu with SIP, especially in the archaeal community. The methanogens represent a small portion of the total microbial communities in Outokumpu deep subsurface, since both the archaeal 16S rRNA and *mcrA* genes have been present only in low copy numbers, and the *mcrA* gene has been detected only from the shallower depths [20,22]. At 2260 m depth, the *mcrA*-genes were not detected with qPCR, with the detection limit being 4×10^1 copies mL⁻¹ fracture fluid [22]. Hence, these prior results indicate that the labelled archaeal taxa represent part of the rare microbial community. Here, we show the archaeal rare biosphere in Outokumpu at a depth of 2.2 km to be an active part of

the microbial community. Acetate amendment enriched rare archaeal taxa which rapidly reacted at the ribosynthesis level to the given substrate. Bacterial players in the acetate linked food-web belonged to the families *Burkholderiaceae* and *Pseudomonadaceae*. The detected ^{13}C -label in the archaeal nucleic acids showed that acetate was actively assimilated by various methanogenic archaea (Figure 3, Table S2). Part of the major acetate assimilating archaea detected in the labelled DNA fractions belonged to the genera *Methanosarcina* spp. and unclassified *Methanosarcinaceae*. *Methanosarcinales* are metabolically the most versatile of the methanogenic archaeal order known to date, with their metabolic capabilities including the disproportioning of acetate, hydrogenotrophic metabolism (H_2/CO_2), and partial oxidation of methyl compounds such as methanol combined with methyl reduction [64,65]. The *Methanosarcina*-related archaeal metabolism is particularly interesting in the deepest part of Outokumpu subsurface, since *Methanosarcina* spp. could represent a flexible key-organism, further supporting the metabolically-more-limited hydrogenotrophic and methylotrophic archaeal taxa. *Methanosarcina* spp., which has previously been detected from the Outokumpu deep biosphere at the upper parts of the bedrock [22]. Purkamo et al. [20] reported a low abundance of *Methanosarcina* spp. at 2260 m depth in Outokumpu, but the archaeal community was, nevertheless, dominated by hydrogenotrophic *Methanobacterium* spp. The genetic potential for aceticlastic methanogenesis has been demonstrated in the Outokumpu deep subsurface at various depths by the presence of *mcrA*-gene and methanogenic microbial genera [21]. Our present study shows that the methanogenic archaeal communities are diverse and active at the deepest parts of the Outokumpu subsurface. *Methanosarcinales* has been detected elsewhere in deep terrestrial subsurfaces, such as in the Evander gold mine in South Africa [16].

The labelled fractions of DNA samples showed a clear rise of the *Methanococcus* spp. affiliating OTUs, demonstrating the presence of the labelled carbon in their nucleic acids. *Methanococcales* has previously been detected from Outokumpu subsurface from the shallower depth of 500 m [66]. The known methanococci-linked abilities indicate that *Methanococcus* spp. utilize acetate as their carbon rather than as an energy source at the depth of 2.2 km in Outokumpu. *Methanococcales* is a methanogenic group of archaea, hydrogenotrophs utilizing hydrogen and carbon dioxide as an energy and carbon source [67,68]. Methanococci can be either heterotrophs or autotrophs possessing different enzymes for initial assimilation of acetate [69]. *Methanococcus voltaii* has been shown to utilize acetate as a source for cellular carbon, despite the usage of formate and H_2 oxidation for energy source through methanogenesis [70]. The *Methanococcus maripaludis* strain S2 utilizes Wood-Ljungdahl-pathway to produce acetyl-CoA from CO_2 molecules, and further uses acetyl-CoA in the production of cell mass or methanogenesis [71]. Furthermore, *Methanococcus* spp. includes known acetate auxotrophs which require acetate for their growth [72]. Study by Ozuolmez et al. [68] revealed the possibilities of a syntrophy between marine aceticlastic archaea and *Methanococcus* spp. in the utilization of acetate. In light of their results, we could make an alternative assumption of cross-feeding in our experiment, with *Methanosarcina* spp. as the original acetate consumer and *Methanococcus* spp. (as a possible syntrophic partner) further scavenging formed hydrogen and $^{13}\text{CO}_2$.

Our study shows *Methanolobus* spp. carrying the heavy ^{13}C -label in DNA. *Methanolobus* spp. has been isolated from the deep subsurface environments, e.g., in Taiwan faults at the depth of 545 m [73] and in deep subsurface coal seams [74]. Known *Methanolobus* spp. are methanogenic archaea producing methane from methylated substrates such as methanol, methylamines, or methyl sulfides [75–77]. However, no *Methanolobus* spp. has been described to grow on acetate [75–77]. Either Outokumpu hosts the first non-obligate methylotrophic methanogenic *Methanolobus* spp. assimilating acetate, or *Methanolobus* spp. is assimilating end-products from the cleavage of acetate ($^{13}\text{CO}_2$) or derivative compounds of $^{13}\text{CH}_4$ oxidation such as methyl sulfides or methanol [78,79]. Methanogenic archaea are able to oxidize methane during active methanogenesis, e.g., *Methanosarcina barkeri* is able to produce methanol and acetate as methane oxidation end-products [79]. Furthermore, *Methanosarcina acetivorans* has been shown to oxidize methane to methyl sulfides or acetate in trace methane oxidation (TMO) experiments [78]. Thus, Moran et al. [78] suggested methyl sulfides as

the intermediates of anaerobic methane oxidation (AOM). Question arises about whether anaerobic (trace) methane oxidation in 2.2 km depth of Outokumpu subsurface by active methanogens could lead to the suitable substrates for *Methanolobus* spp., and in this experiment to precursors with labelled C. Furthermore, the methylotrophic and acetoclastic methanogenesis linked genes were detected at the depth of 2300 m from Outokumpu metagenome, and methanol was suggested as a possible reduced C-1 substrate for methylotrophic methanogens [11]. The presence of both *Methanosarcina* spp. and *Methanolobus* spp. demonstrate potential for methylotrophic methanogenesis at the depth of 2.2 km, and this study shows *Methanolobus* spp. taking active part in deep terrestrial carbon cycling in Outokumpu.

One of the enrichment RNA samples shows the activation and ribosomal response to acetate amendment by the similar genera to DNA samples including *Methanosarcina* spp., *Methanolobus* spp., and unclassified *Methanosarcinaceae*. The RNA samples host labelled *Methanothermobacter* spp. and *Methanobacterium* spp. affiliating OTUs, demonstrating rapid archaeal response. *Methanothermobacter* spp. are thermophilic hydrogenotrophic methanogenic archaea capable of reducing CO₂ to CH₄, along with H₂ as an electron donor [80,81]. In addition, some of the *Methanothermobacter* species have been suggested to be able to assimilate acetate [81]. Interestingly, the firstly activated archaeal genera *Methanothermobacter* spp. are missing from the labelled DNA samples representing a later, more stable time-point. This could indicate that *Methanothermobacter* spp. are not able to compete with other archaea long-term, and that incubation conditions favour the other acetate assimilating archaea. The *Methanothermobacter wolfeii* spp. type strain has been shown to lyse in the energy deprivation state [81]. *Methanobacterium* spp. has been described as the dominant archaeal taxa represented throughout the Outokumpu bedrock fracture zones [11,20].

In the present study, the major bacterial families observed with labelled carbon in their nucleic acids belonged to the *Pseudomonadaceae* and *Burkholderiaceae*. The labelled fractions hosted a diversity of OTUs within the *Burkholderiaceae*, but did not clearly demonstrate one genus linked to the acetate amendment. Hence, this could possibly indicate partial labelling of the bacterial nucleic acids, or archaea more actively scavenging labelled carbon compounds. Part of the bacterial community could be labelled in response to utilization of the labelled ¹³CO₂ formed in acetoclastic methanogenesis by *Methanosarcina* spp. The bacterial genera observed with labelled nucleic acids have been shown to compete efficiently for their niche in the microbial communities in various nutrient-poor environments [82]. In the Outokumpu deep biosphere, the *Burkholderiales* have been described as a keystone species [22]. *Pseudomonas* spp. represents one of the core community genera in Outokumpu subsurface at the majority of the studied depths, and the family *Pseudomonadaceae* covered 25% of the total OTUs detected at the depth of 2300 m [22]. Furthermore, incorporation of the inorganic carbonate-C into cell structures by carbon fixation was observed with both *Burkholderia* spp. and *Pseudomonas* spp. isolates from the Outokumpu shallow depth of 180 m [83]. *Burkholderia* spp. and *Pseudomonas* spp. represent part of the abundant taxa in other deep subsurface environments, e.g., in Äspö, Sweden [84]. In addition, *Pseudomonas* spp. has been detected from Río Tinto rock core enrichments with H₂/CO₂ atmosphere [85]. In our study, the *Pseudomonas* spp. could present the carbon fixating partner or benefiter coupled to archaeal acetate assimilation. However, the labelled archaeal genera can similarly target the carbon dioxide produced by *Methanosarcina* spp. metabolism. *Pseudomonas* spp. could represent a genus capable of adjusting its metabolism, thus possibly competing for the resources more efficiently when nutrients become available in a deep biosphere. One of the major genera detected within *Burkholderiaceae* was *Comamonas* spp. in the labelled DNA samples. Environmental isolates of *Comamonas* spp. have been shown to grow on acetate [86,87]. Therefore, the labelling of *Comamonas* spp. could indicate acetate consumption in deep terrestrial biospheres. *Comamonadaceae* from deep subsurface environments have been suggested to use extracellular electron transfer (EET), in which the electrons from the donor, such as acetate, are transferred to external surfaces [88]. Jangir et al. [88] suggest that in deep subsurface environments, the insoluble mineral surfaces could offer an electron sink, thus increasing the prospective metabolism routes and redox

couples for the subsurface microbial communities. The detected labelled genera such as *Duganella* spp., belonging to the family *Burkholderiaceae*, have previously been detected as contaminants in molecular biology kits [60]. However, in DNA and RNA experiments, the enriched samples hosted 0.0–33.3% and labelled DNA samples 0.0–13.4% of unclassified *Burkholderiaceae* affiliating sequences (Table S3). Thus, these taxa could be interpreted as intrinsic, previously unclassified deep subsurface taxa, rather than contaminants arising from the reagents. The enriched RNA samples hosted a variety of human related contaminants such as *Streptococcus* spp., and were not considered as possible deep subsurface genera (Table S4). These contaminants were likely detected as cDNA samples hosting small amounts of nucleic acids went through the WGA prior to amplicon library PCR.

SIP targeting the acetate-assimilating communities revealed the suitability of the modified filter-concentration C-SIP method for saline, low biomass subsurface fluids. However, this method could have underestimated the role of small-sized subsurface cells passing the 0.22 µm pore size filters [61,89]. The SIP method relies on the ability of the microorganisms to actively metabolize these, given heavy isotope-labelled substrates. However, the exact environmental conditions, such as the pressure or constant gas exchange, of deep biospheres are not replicable in laboratory microcosms. The SIP method produces a bias missing the species that are profoundly dependent on such conditions. Nevertheless, SIP presents an effective, molecular-based metabolism studying tool which is not dependent on growth as much as on cell-level reactions [35]. These reactions require the synthesis and transfer of labelled carbon to nucleic acids in adequate levels to allow the separation from un-labelled background nucleic acids [42,90]. In our study, we investigated the acetate cycling with DNA SIP, and RNA-targeted cell activation. The previous study from Outokumpu showed the fast activation of dormant cells in the presence of C-1 compounds [91]. A further study by Rajala and Bomberg [66] demonstrated the similar response to C-1 compounds on RNA level, indicating that our incubation time of three hours was sufficient with regards to the RNA synthesis. The rise of proteobacterial OTUs during the incubation in enriched and labelled samples shows the activation of the bacterial communities. The DNA and RNA results support each other, thus strengthening the notions made on acetate cycling and characterization of the actual active communities.

5. Conclusions

Methanosarcina spp. and *Methanococcus* spp., along with unclassified *Methanosarcinaceae* genera, have the potential to assimilate acetate at the depth of 2.2 km in Outokumpu. Archaeal genera *Methanococcus* spp. and *Methanolobus* spp. were active in the food-web linked to the acetate. Based on the detected archaeal genera, Outokumpu deep biosphere has the potential for biotic methane formation by hydrogenotrophic, acetoclastic, and methylotrophic methanogenesis pathways at the depth of 2.2 km. Outokumpu deep subsurface microorganisms responded very rapidly to amended compounds, resulting in both cell activation and RNA synthesis. In addition, the activation of archaea enriched the detected species diversity. *Methanothermobacter* spp. was observed from the Outokumpu subsurface for the first time, and *Methanococcus* spp., *Methanolobus* spp., *Methanosarcina* spp., and unclassified *Methanosarcinaceae* were detected from 2.2 km depth for the first time. DNA SIP was confirmed to be applicable for this kind of saline low biomass fracture fluids, with filter concentration modifications.

Outokumpu deep subsurface hosts a high number of different unknown taxa and unclassified OTUs, leaving the metabolic abilities of the microbial communities at deeper depths still to be explored. The potential of methylated substrates and methylotrophic methanogenesis in the deepest part of Outokumpu subsurface could be further studied.

Supplementary Materials: The following are available online at <http://www.mdpi.com/2076-3263/8/11/418/s1>, Figure S1 Relative bacterial 16S rRNA gene ratios recovered from CsCl gradient fractions from ¹²C and ¹³C DNA samples, Table S1. PCR mixes for archaeal and bacterial 16S rRNA gene amplicon library PCR, Table S2. Archaeal 16S rRNA gene OTU taxonomy, Table S3. Bacterial 16S rRNA gene OTU taxonomy, DNA samples, Table S4. Bacterial 16S rRNA gene OTU taxonomy, RNA samples.

Author Contributions: M.N.-P. conceived and designed the experiments, performed the experiments, analyzed the data and wrote the paper. L.P. and M.N. designed the experiments and wrote the paper; R.K. wrote the paper; M.I., L.A. and I.K.: project administration, funding acquisition and contribution with scientific discussions and comments; R.K., L.A. and I.K.: geochemistry; M.B. conceived and designed the experiments, analyzed the data, wrote the paper and supervised the work. All authors commented the data and the manuscript.

Funding: This research was funded by The Academy of Finland (DEEP LIFE project, grant no. 133348/2009) and the Finnish Research Program on Nuclear Waste Management. Ella and Georg Ehrnrooth Foundation, Scholar Fund of Wiipurilainen osakunta and Finnish Concordia Fund are all thanked for research grant.

Acknowledgments: Mirva Pyrhönen from VTT Technical Research Centre of Finland Ltd., is thanked for her skillful laboratory assistance. Arto Pullinen from The Geological Survey of Finland is thanked for helping during the field sampling in Outokumpu. Verona Vandieken is thanked for her time and discussion on SIP methods at SDU, Denmark.

Conflicts of Interest: The authors declare no conflict of interest. The founding sponsors had no role in the design of the study; in the collection, analyses, or interpretation of data; in the writing of the manuscript, and in the decision to publish the results.

References

1. Magnabosco, C.; Lin, L.-H.; Dong, H.; Bomberg, M.; Ghiorse, W.; Stan-Lotter, H.; Pedersen, K.; Kieft, T.L.; Onstott, T.C. The Biomass and Biodiversity of the Continental Subsurface. *Nat. Geosci.* **2018**. [[CrossRef](#)]
2. McMahon, S.; Parnell, J. Weighing the deep continental biosphere. *FEMS Microbiol. Ecol.* **2014**, *87*, 113–120. [[CrossRef](#)] [[PubMed](#)]
3. Whitman, W.B.; Coleman, D.C.; Wiebe, W.J. Prokaryotes: The unseen majority. *Proc. Natl. Acad. Sci. USA* **1998**, *95*, 6578–6583. [[CrossRef](#)] [[PubMed](#)]
4. Kotelnikova, S.; Pedersen, K. Evidence for methanogenic *Archaea* and homoacetogenic *Bacteria* in deep granitic rock aquifers. *FEMS Microbiol. Rev.* **1997**, *20*, 339–349. [[CrossRef](#)]
5. Pedersen, K. Microbial life in deep granitic rock. *FEMS Microbiol. Rev.* **1997**, *20*, 399–414. [[CrossRef](#)]
6. Lin, L.H.; Hall, J.; Lippmann-Pipke, J.; Ward, J.A.; Lollar, B.S.; DeFlaun, M.; Rothmel, R.; Moser, D.; Gihring, T.M.; Mislouack, B.; et al. Radiolytic H₂ in continental crust: Nuclear power for deep subsurface microbial communities. *Geochim. Geophys. Geosyst.* **2005**, *6*. [[CrossRef](#)]
7. Lin, L.H.; Slater, G.F.; Sherwood Lollar, B.; Lacrampe-Couloume, G.; Onstott, T.C. The yield and isotopic composition of radiolytic H₂, a potential energy source for the deep subsurface biosphere. *Geochim. Cosmochim. Acta* **2005**, *69*, 893–903. [[CrossRef](#)]
8. Kietäväinen, R.; Purkamo, L. The origin, source, and cycling of methane in deep crystalline rock biosphere. *Front. Microbiol.* **2015**, *6*. [[CrossRef](#)] [[PubMed](#)]
9. Kotelnikova, S. Microbial production and oxidation of methane in deep subsurface. *Earth-Sci. Rev.* **2002**, *58*, 367–395. [[CrossRef](#)]
10. Ward, J.A.; Slater, G.F.; Moser, D.P.; Lin, L.H.; Lacrampe-Couloume, G.; Bonin, A.S.; Davidson, M.; Hall, J.A.; Mislouack, B.; Bellamy, R.E.S.; et al. Microbial hydrocarbon gases in the Witwatersrand Basin, South Africa: Implications for the deep biosphere. *Geochim. Cosmochim. Acta* **2004**, *68*, 3239–3250. [[CrossRef](#)]
11. Nyysönen, M.; Hultman, J.; Ahonen, L.; Kukkonen, I.; Paulin, L.; Laine, P.; Itävaara, M.; Auvinen, P. Taxonomically and functionally diverse microbial communities in deep crystalline rocks of the Fennoscandian shield. *ISME J.* **2014**, *8*, 126–138. [[CrossRef](#)] [[PubMed](#)]
12. Ino, K.; HERNSDORF, A.W.; KONNO, U.; Kouduka, M.; Yanagawa, K.; Kato, S.; Sunamura, M.; Hirota, A.; Togo, Y.S.; Ito, K.; et al. Ecological and genomic profiling of anaerobic methane-oxidizing archaea in a deep granitic environment. *ISME J.* **2018**, *12*, 31–47. [[CrossRef](#)] [[PubMed](#)]
13. Lever, M.A. Acetogenesis in the energy-starved deep biosphere—a paradox? *Front. Microbiol.* **2012**, *2*, 1–18. [[CrossRef](#)] [[PubMed](#)]
14. Haveman, S.A.; Pedersen, K.; Ruotsalainen, P. Distribution and metabolic diversity of microorganisms in deep igneous rock aquifers of Finland. *Geomicrobiol. J.* **1999**, *16*, 277–294. [[CrossRef](#)]
15. Chivian, D.; Brodie, E.L.; Alm, E.J.; Culley, D.E.; Dehal, P.S.; DeSantis, T.Z.; Gihring, T.M.; Lapidus, A.; Lin, L.-H.; Lowry, S.R.; et al. Environmental Genomics Reveals a Single-Species Ecosystem Deep Within Earth. *Science* **2008**, *322*, 275–278. [[CrossRef](#)] [[PubMed](#)]

16. Davidson, M.M.; Silver, B.J.; Onstott, T.C.; Moser, D.P.; Gihring, T.M.; Pratt, L.M.; Boice, E.A.; Lollar, B.S.; Lippmann-Pipke, J.; Pfiffner, S.M.; et al. Capture of Planktonic Microbial Diversity in Fractures by Long-Term Monitoring of Flowing Boreholes, Evander Basin, South Africa. *Geomicrobiol. J.* **2011**, *28*, 275–300. [[CrossRef](#)]
17. Lau, M.C.Y.; Kieft, T.L.; Kuloyo, O.; Linage-Alvarez, B.; Van Heerden, E. An oligotrophic deep-subsurface community dependent on syntrophy is dominated by sulfur-driven autotrophic denitrifiers. *Proc. Natl. Acad. Sci. USA* **2016**, *113*, E7927–E7936. [[CrossRef](#)] [[PubMed](#)]
18. Itävaara, M.; Nyyssönen, M.; Kapanen, A.; Nousiainen, A.; Ahonen, L.; Kukkonen, I. Characterization of bacterial diversity to a depth of 1500 m in the Outokumpu deep borehole, Fennoscandian Shield. *FEMS Microbiol. Ecol.* **2011**, *77*, 295–309. [[CrossRef](#)] [[PubMed](#)]
19. Sharma, P.; Tsang, C.F.; Kukkonen, I.T.; Niemi, A. Analysis of 6-year fluid electric conductivity logs to evaluate the hydraulic structure of the deep drill hole at Outokumpu, Finland. *Int. J. Earth Sci.* **2016**, *105*, 1549–1562. [[CrossRef](#)]
20. Purkamo, L.; Bomberg, M.; Nyyssönen, M.; Kukkonen, I.; Ahonen, L.; Kietäväinen, R.; Itävaara, M. Dissecting the deep biosphere: Retrieving authentic microbial communities from packer-isolated deep crystalline bedrock fracture zones. *FEMS Microbiol. Ecol.* **2013**, *85*, 324–337. [[CrossRef](#)] [[PubMed](#)]
21. Purkamo, L.; Bomberg, M.; Nyyssönen, M. Heterotrophic Communities Supplied by Ancient Organic Carbon Predominate in Deep Fennoscandian Bedrock Fluids. *Microb. Ecol.* **2015**, 319–332. [[CrossRef](#)] [[PubMed](#)]
22. Purkamo, L.; Bomberg, M.; Kietäväinen, R.; Salavirta, H.; Nyyssönen, M.; Nuppunen-Puputti, M.; Ahonen, L.; Kukkonen, I.; Itävaara, M. Microbial co-occurrence patterns in deep Precambrian bedrock fracture fluids. *Biogeosciences* **2016**, *13*. [[CrossRef](#)]
23. Ahonen, L.; Kietäväinen, R.; Kortelainen, N.; Kukkonen, I.T.; Pullinen, A.; Toppi, T.; Bomberg, M.; Itävaara, M.; Nousiainen, A.; Nyyssönen, M.; Öster, M. Hydrogeological characteristics of the Outokumpu Deep Drill Hole. *Spec. Pap. Geol. Surv. Finl.* **2011**, *2011*, 151–168.
24. Kukkonen, I.T.; Rath, V.; Kivekäs, L.; Šafanda, J.; Čermak, V. Geothermal studies of the Outokumpu Deep Drill Hole, Finland: Vertical variation in heat flow and palaeoclimatic implications. *Phys. Earth Planet. Inter.* **2011**, *188*, 9–25. [[CrossRef](#)]
25. Kietäväinen, R.; Ahonen, L.; Kukkonen, I.T.; Hendriksson, N.; Nyyssönen, M.; Itävaara, M. Characterisation and isotopic evolution of saline waters of the Outokumpu Deep Drill Hole, Finland—Implications for water origin and deep terrestrial biosphere. *Appl. Geochem.* **2013**, *32*, 37–51. [[CrossRef](#)]
26. Kietäväinen, R.; Ahonen, L.; Niinikoski, P.; Nykänen, H.; Kukkonen, I.T. Abiotic and biotic controls on methane formation down to 2.5 km depth within the Precambrian Fennoscandian Shield. *Geochim. Cosmochim. Acta* **2017**, *202*, 124–145. [[CrossRef](#)]
27. Kietäväinen, R.; Ahonen, L.; Kukkonen, I.T.; Niedermann, S.; Wiersberg, T. Noble gas residence times of saline waters within crystalline bedrock, Outokumpu Deep Drill Hole, Finland. *Geochim. Cosmochim. Acta* **2014**, *145*, 159–174. [[CrossRef](#)]
28. Magnabosco, C.; Ryan, K.; Lau, M.C.Y.; Kuloyo, O.; Sherwood Lollar, B.; Kieft, T.L.; Van Heerden, E.; Onstott, T.C. A metagenomic window into carbon metabolism at 3 km depth in Precambrian continental crust. *ISME J.* **2016**, *10*, 730–741. [[CrossRef](#)] [[PubMed](#)]
29. Borrel, G.; Adam, P.S.; Gribaldo, S. Methanogenesis and the Wood-Ljungdahl pathway: An ancient, versatile, and fragile association. *Genome Biol. Evol.* **2016**, evw114. [[CrossRef](#)] [[PubMed](#)]
30. Purkamo, L.; Bomberg, M.; Nyyssönen, M.; Ahonen, L.; Kukkonen, I.; Itävaara, M. Response of deep subsurface microbial community to different carbon sources and electron acceptors during ~2 months incubation in microcosms. *Front. Microbiol.* **2017**, *8*. [[CrossRef](#)] [[PubMed](#)]
31. Pedersen, K.; Arlinger, J.; Eriksson, S.; Hallbeck, A.; Hallbeck, L.; Johansson, J. Numbers, biomass and cultivable diversity of microbial populations relate to depth and borehole-specific conditions in groundwater from depths of 4–450 m in Olkiluoto, Finland. *ISME J.* **2008**, *2*, 760–775. [[CrossRef](#)] [[PubMed](#)]
32. Kotelnikova, S.; Pedersen, K. Distribution and activity of methanogens and homoacetogens in deep granitic aquifers at Äspö Hard Rock Laboratory, Sweden. *FEMS Microbiol. Ecol.* **1998**, *26*, 121–134. [[CrossRef](#)]
33. Shock, E.L.; Schulte, M.D. Organic synthesis during fluid mixing in hydrothermal systems. *J. Geophys. Res. Planets* **1998**, *103*, 28513–28527. [[CrossRef](#)]
34. Radajewski, S.; Ineson, P.; Parekh, N.R.; Murrell, J.C. Stable isotope probing as a tool in microbial ecology. *Nature* **2000**, *403*, 646–649. [[CrossRef](#)] [[PubMed](#)]

35. Lueders, T.; Dumont, M.G.; Bradford, L.; Manefield, M. RNA-stable isotope probing: From carbon flow within key microbiota to targeted transcriptomes. *Curr. Opin. Biotechnol.* **2016**, *41*, 83–89. [[CrossRef](#)] [[PubMed](#)]
36. Bombach, P.; Chatzinotas, A.; Neu, T.R.; Kästner, M.; Lueders, T.; Vogt, C. Enrichment and characterization of a sulfate-reducing toluene-degrading microbial consortium by combining in situ microcosms and stable isotope probing techniques. *FEMS Microbiol. Ecol.* **2010**, *71*, 237–246. [[CrossRef](#)] [[PubMed](#)]
37. Pilloni, G.; von Netzer, F.; Engel, M.; Lueders, T. Electron acceptor-dependent identification of key anaerobic toluene degraders at a tar-oil-contaminated aquifer by Pyro-SIP. *FEMS Microbiol. Ecol.* **2011**, *78*, 165–175. [[CrossRef](#)] [[PubMed](#)]
38. Beckmann, S.; Lueders, T.; Krüger, M.; von Netzer, F.; Engelen, B.; Cypionka, H. Acetogens and acetoclastic Methanosarcinales govern methane formation in abandoned coal mines. *Appl. Environ. Microbiol.* **2011**, *77*, 3749–3756. [[CrossRef](#)] [[PubMed](#)]
39. Na, H.; Lever, M.A.; Kjeldsen, K.U.; Schulz, F.; Jørgensen, B.B. Uncultured Desulfobacteraceae and Crenarchaeotal group C3 incorporate ¹³C-acetate in coastal marine sediment. *Environ. Microbiol. Rep.* **2015**, *7*, 614–622. [[CrossRef](#)] [[PubMed](#)]
40. Kietäväinen, R. *Deep Groundwater Evolution at Outokumpu, Eastern Finland: From Meteoric Water to Saline Gas-Rich Fluid*; Special Publication 97; Geological Survey of Finland: Espoo, Finland, 2017; p. 37. ISBN 978-952-217-375-1.
41. Västi, K. Petrology of the drill hole R2500 at Outokumpu, Eastern Finland—The deepest drill hole ever drilled in Finland. In *Outokumpu Deep Drilling Project 2003–2010*; Kukkonen, I.T., Ed.; Special Paper 33; Geological Survey of Finland: Espoo, Finland, 2011; pp. 197–210. ISBN 9789522171528.
42. Neufeld, J.D.; Vohra, J.; Dumont, M.G.; Lueders, T.; Manefield, M.; Friedrich, M.W.; Murrell, J.C. DNA stable-isotope probing. *Nat. Protoc.* **2007**, *2*, 860–866. [[CrossRef](#)] [[PubMed](#)]
43. Weisburg, W.G.; Barns, S.M.; Pelletier, D.A.; Lane, D.J. 16S ribosomal DNA amplification for phylogenetic study. *J. Bacteriol.* **1991**, *173*, 697–703. [[CrossRef](#)] [[PubMed](#)]
44. Muyzer, G.; de Waal, E.; Uitterlinden, A.G. Profiling of complex microbial populations by denaturing gradient gel electrophoresis analysis of polymerase chain reaction-amplified genes coding for 16S rRNA. *Appl. Environ. Microbiol.* **1993**, *59*, 695–700. [[PubMed](#)]
45. Edwards, U.; Rogall, T.; Blöcker, H.; Emde, M.; Böttger, E.C. Isolation and direct complete nucleotide determination of entire genes. Characterization of a gene coding for 16S ribosomal RNA. *Nucleic Acids Res.* **1989**, *17*, 7843–7853. [[CrossRef](#)] [[PubMed](#)]
46. Großkopf, R.; Janssen, P.H.; Liesack, W. Diversity and structure of the methanogenic community in anoxic rice paddy soil microcosms as examined by cultivation and direct 16S rRNA gene sequence retrieval. *Appl. Environ. Microbiol.* **1998**, *64*, 960–969. [[PubMed](#)]
47. Stahl, A.D.; Amann, R. Development and Application of Nucleic Acid Probes. In *Nucleic Acid Techniques in Bacterial Systematics*; Stackebrandt, E., Goodfellow, M., Eds.; John Wiley & Sons Ltd.: New York, NY, USA, 1991; pp. 205–248. ISBN 0471929069.
48. Bano, N.; Ruffin, S.; Ransom, B.; Hollibaugh, J.T. Phylogenetic Composition of Arctic Ocean Archaeal Assemblages and Comparison with Antarctic Assemblages. *Appl. Environ. Microbiol.* **2004**, *70*, 781–789. [[CrossRef](#)] [[PubMed](#)]
49. Barns, S.M.; Fundyga, R.E.; Jeffries, M.W.; Pace, N.R. Remarkable archaeal diversity detected in a Yellowstone National Park hot spring environment (archaeobacteria/phylogeny/thermophly/molecular ecology). *Proc. Natl. Acad. Sci. USA* **1994**, *91*, 1609–1613. [[CrossRef](#)] [[PubMed](#)]
50. Bomberg, M.; Nyyssönen, M.; Pitkänen, P.; Lehtinen, A.; Itävaara, M. Active Microbial Communities Inhabit Sulphate-Methane Interphase in Deep Bedrock Fracture Fluids in Olkiluoto, Finland. *Biomed. Res. Int.* **2015**, *2015*. [[CrossRef](#)] [[PubMed](#)]
51. Schloss, P.D.; Westcott, S.L.; Ryabin, T.; Hall, J.R.; Hartmann, M.; Hollister, E.B.; Lesniewski, R.A.; Oakley, B.B.; Parks, D.H.; Robinson, C.J.; et al. Introducing mothur: Open-source, platform-independent, community-supported software for describing and comparing microbial communities. *Appl. Environ. Microbiol.* **2009**, *75*, 7537–7541. [[CrossRef](#)] [[PubMed](#)]
52. Quast, C.; Pruesse, E.; Yilmaz, P.; Gerken, J.; Schweer, T.; Yarza, P.; Peplies, J.; Glöckner, F.O. The SILVA ribosomal RNA gene database project: Improved data processing and web-based tools. *Nucleic Acids Res.* **2012**, *41*, D590–D596. [[CrossRef](#)] [[PubMed](#)]
53. Altschul, S.F.; Gish, W.; Miller, W.; Myers, E.W.; Lipman, D.J. Basic local alignment search tool. *J. Mol. Biol.* **1990**, *215*, 403–410. [[CrossRef](#)]

54. RStudio Team. RStudio: Integrated Development for R. 2015. Available online: <http://www.rstudio.com/> (accessed on 13 November 2018).
55. Paulson, J.N.; Talukder, H.; Pop, M.; Bravo, H.C. MetagenomeSeq: Statistical Analysis for Sparse High-Throughput Sequencing. *Bioconductor* **2013**. [[CrossRef](#)]
56. McMurdie, P.J.; Holmes, S. phyloseq: An R Package for Reproducible Interactive Analysis and Graphics of Microbiome Census Data. *PLoS ONE* **2013**, *8*, e61217. [[CrossRef](#)] [[PubMed](#)]
57. Oksanen, J.; Blanchet, F.G.; Friendly, M.; Kindt, R.; Legendre, P.; Mcglinn, D.; Minchin, P.R.; O'hara, R.B.; Simpson, G.L.; Solymos, P.; et al. Package "vegan" Title Community Ecology Package. 2018. Available online: <https://cran.r-project.org/web/packages/vegan/vegan.pdf>; <https://cran.r-project.org/>; <https://github.com/vegandevs/vegan> (accessed on 13 November 2018).
58. Tardy-Jacquenod, C.; Magot, M.; Patel, B.K.C.; Matheron, R.; Caumette, P. *Desulfotomaculum halophilum* sp. nov., a halophilic sulfate-reducing bacterium isolated from oil production facilities. *Int. J. Syst. Bacteriol.* **1998**, *48*, 333–338. [[CrossRef](#)] [[PubMed](#)]
59. Sheik, C.S.; Reese, B.K.; Twing, K.I.; Sylvan, J.B.; Grim, S.L.; Schrenk, M.O.; Sogin, M.L.; Colwell, F.S.; Emerson, D. Identification and Removal of Contaminant Sequences From Ribosomal Gene Databases: Lessons From the Census of Deep Life. *Front. Microbiol.* **2018**, *9*, 840. [[CrossRef](#)] [[PubMed](#)]
60. Salter, S.J.; Cox, M.J.; Turek, E.M.; Calus, S.T.; Cookson, W.O.; Moffatt, M.F.; Turner, P.; Parkhill, J.; Loman, N.J.; Walker, A.W. Reagent and laboratory contamination can critically impact sequence-based microbiome analyses. *BMC Biol.* **2014**, *12*, 87. [[CrossRef](#)] [[PubMed](#)]
61. Wu, X.; Holmfeldt, K.; Hubalek, V.; Lundin, D.; Åström, M.; Bertilsson, S.; Dopson, M. Microbial metagenomes from three aquifers in the Fennoscandian shield terrestrial deep biosphere reveal metabolic partitioning among populations. *ISME J.* **2016**, *10*, 1192–1203. [[CrossRef](#)] [[PubMed](#)]
62. Hallbeck, L.; Pedersen, K. Culture-dependent comparison of microbial diversity in deep granitic groundwater from two sites considered for a Swedish final repository of spent nuclear fuel. *FEMS Microbiol. Ecol.* **2012**, *81*, 66–77. [[CrossRef](#)] [[PubMed](#)]
63. Haveman, S.A.; Nilsson, E.; Pedersen, K. *Regional distribution of microbes in groundwater from Håstholmen, Kievetty, Olkiluoto and Romuvaara, Finland*; POSIVA Ltd.: Helsinki, Finland, 2000; ISBN 9516520928.
64. Lang, K.; Schuldes, J.; Klingl, A.; Poehlein, A.; Daniel, R.; Brune, A. New mode of energy metabolism in the seventh order of methanogens as revealed by comparative genome analysis of "Candidatus Methanoplasma termitum". *Appl. Environ. Microbiol.* **2015**, *81*, 1338–1352. [[CrossRef](#)] [[PubMed](#)]
65. Bapteste, É.; Brochier, C.; Boucher, Y. Higher-level classification of the Archaea: Evolution of methanogenesis and methanogens. *Archaea* **2005**, *1*, 353–363. [[CrossRef](#)] [[PubMed](#)]
66. Rajala, P.; Bomberg, M. Reactivation of Deep Subsurface Microbial Community in Response to Methane or Methanol Amendment. *Front. Microbiol.* **2017**, *8*, 431. [[CrossRef](#)] [[PubMed](#)]
67. Jones, W.J.; Paynter, M.J.B.; Gupta, R. Microbiology 9. *Arch. Microbiol.* **1983**, *135*, 91–97. [[CrossRef](#)]
68. Ozuolmez, D.; Na, H.; Lever, M.A.; Kjeldsen, K.U.; Jørgensen, B.B.; Plugge, C.M. Methanogenic archaea and sulfate reducing bacteria co-cultured on acetate: Teamwork or coexistence? *Front. Microbiol.* **2015**, *6*, 492. [[CrossRef](#)] [[PubMed](#)]
69. Shieh, J.; Whitman, W.B. Pathway of Acetate Assimilation in Autotrophic and Heterotrophic Methanococci. *J. Bacteriol.* **1987**, *169*, 5327–5329. [[CrossRef](#)] [[PubMed](#)]
70. Whitman, W.B.; Ankwanda, E.; Wolfe, R.S. Nutrition and carbon metabolism of Methanococcus-Voltae. *J. Bacteriol.* **1982**, *149*, 852–863. [[PubMed](#)]
71. Goyal, N.; Widiastuti, H.; Karimi, I.A.; Zhou, Z. A genome-scale metabolic model of Methanococcus maripaludis S2 for CO₂ capture and conversion to methane. *Mol. BioSyst.* **2014**, *10*, 1043–1054. [[CrossRef](#)] [[PubMed](#)]
72. Ladapo, J.; Whitman, W.B. Method for isolation of auxotrophs in the methanogenic archaeobacteria: Role of the acetyl-CoA pathway of autotrophic CO₂ fixation in Methanococcus maripaludis. *Proc. Natl. Acad. Sci. USA* **1990**, *87*, 5598–5602. [[CrossRef](#)] [[PubMed](#)]
73. Wu, S.; Lai, M. Methanogenic Archaea Isolated from Taiwan's Chelungpu Fault. *Appl. Environ. Microbiol.* **2011**, *77*, 830–838. [[CrossRef](#)] [[PubMed](#)]
74. Doerfert, S.N.; Reichlen, M.; Iyer, P.; Wang, M.; Ferry, J.G. *Methanobolus zinderi* sp. nov., a methylotrophic methanogen isolated from a deep subsurface coal seam. *Int. J. Syst. Evol. Microbiol.* **2009**, *59*, 1064–1069. [[CrossRef](#)] [[PubMed](#)]

75. Oremland, R.S.; Boone, D.R. NOTES: *Methanobolus taylorii* sp. nov., a New Methylophilic, Estuarine Methanogen. *Int. J. Syst. Bacteriol.* **1994**, *44*, 573–575. [[CrossRef](#)]
76. Mochimaru, H.; Tamaki, H.; Hanada, S.; Imachi, H.; Nakamura, K.; Sakata, S.; Kamagata, Y. *Methanobolus profundi* sp. nov., a methylophilic methanogen isolated from deep subsurface sediments in a natural gas field. *Int. J. Syst. Evol. Microbiol.* **2009**, *59*, 714–718. [[CrossRef](#)] [[PubMed](#)]
77. Zhang, G.; Jiang, N.; Liu, X.; Dong, X. Methanogenesis from methanol at low temperatures by a novel psychrophilic methanogen, “*Methanobolus psychrophilus*” sp. nov., prevalent in Zoige wetland of the Tibetan plateau. *Appl. Environ. Microbiol.* **2008**, *74*, 6114–6120. [[CrossRef](#)] [[PubMed](#)]
78. Moran, J.J.; House, C.H.; Thomas, B.; Freeman, K.H. Products of trace methane oxidation during nonmethylophilic growth by *Methanosarcina*. *J. Geophys. Res. Biogeosci.* **2007**, *112*. [[CrossRef](#)]
79. Zehnder, A.J.B.; Brock, T.D. Methane Formation and Methane Oxidation by Methanogenic Bacteria. *J. Bacteriol.* **1979**, *137*, 420–432. [[PubMed](#)]
80. Boone, D.R.; Brenner, D.J.; Castenholz, R.W.; De Vos, P.; Garrity, G.M.; Krieg, N.R.; Goodfellow, M. *Bergey's Manual of Systematic Bacteriology*; Springer: Berlin, Germany, 2001; ISBN 038721609X.
81. Wasserfallen, A.; Nolling, J.; Pfister, P.; Reeve, J.; Conway de Macario, E. Phylogenetic analysis of 18 thermophilic *Methanobacterium* isolates supports the proposals to create a new genus, *Methanothermobacter* gen. nov., and to reclassify several isolates in three species, *Methanothermobacter thermautotrophicus* comb. nov., *Methanothermobacter wolfeii* comb. nov., and *Methanothermobacter marburgensis* sp. nov. *Int. J. Syst. Evol. Microbiol.* **2000**, *50*, 43–53. [[CrossRef](#)] [[PubMed](#)]
82. Compant, S.; Nowak, J.; Coenye, T.; Clément, C.; Ait Barka, E. Diversity and occurrence of *Burkholderia* spp. in the natural environment. *FEMS Microbiol. Rev.* **2008**, *32*, 607–626. [[CrossRef](#)] [[PubMed](#)]
83. Bomberg, M.; Raulio, M.; Jylhä, S.W.; Mueller, C.; Höschen, C.; Rajala, P.; Purkamo, L.; Kietäväinen, R.; Ahonen, L.; Itävaara, M. CO₂ and carbonate as substrate for the activation of the microbial community in 180 m deep bedrock fracture fluid of Outokumpu Deep Drill Hole, Finland. *AIMS Microbiol.* **2017**, *3*, 846–871. [[CrossRef](#)]
84. Hubalek, V.; Wu, X.; Eiler, A.; Buck, M.; Heim, C.; Dopson, M.; Bertilsson, S.; Ionescu, D. Connectivity to the surface determines diversity patterns in subsurface aquifers of the Fennoscandian shield. *ISME J.* **2016**, *2447–2458*. [[CrossRef](#)] [[PubMed](#)]
85. Leandro, T.; Rodriguez, N.; Rojas, P.; Sanz, J.L.; da Costa, M.S.; Amils, R. Study of methanogenic enrichment cultures of rock cores from the deep subsurface of the Iberian Pyritic Belt. *Heliyon* **2018**, *4*. [[CrossRef](#)] [[PubMed](#)]
86. Etchebehere, C.; Errazquin, M.I.; Dabert, P.; Moletta, R.; Muxi, L. *Comamonas nitrivorans* sp. nov., a novel denitrifier isolated from a denitrifying reactor treating landfill leachate. *Int. J. Syst. Evol. Microbiol.* **2001**, *51*, 977–983. [[CrossRef](#)] [[PubMed](#)]
87. De Vos, P.; Kersters, K.; Falsen, E.; Pot, B.; Gillis, M.; Segers, P.; De Ley, J. *Comamonas Davis* and *Park* 1962 gen. nov., norm. rev. emend., and *Comamonas terrigena* Hugh 1962 sp. nov., norm. rev. *Int. J. Syst. Bacteriol.* **1985**, *1956*, 443–453. [[CrossRef](#)]
88. Jangir, Y.; French, S.; Momper, L.M.; Moser, D.P.; Amend, J.P.; El-naggar, M.Y.; Dillon, J.G.; Morgan, H.; Moyer, C.L. Isolation and Characterization of Electrochemically Active Subsurface Delftia and Azonexus Species. *Front. Microbiol.* **2016**, *7*, 756. [[CrossRef](#)] [[PubMed](#)]
89. Comolli, L.R.; Baker, B.J.; Downing, K.H.; Siegerist, C.E.; Banfield, J.F. Three-dimensional analysis of the structure and ecology of a novel, ultra-small archaeon. *ISME J.* **2009**, *3*, 159–167. [[CrossRef](#)] [[PubMed](#)]
90. Neufeld, J.D.; Dumont, M.G.; Vohra, J.; Murrell, J.C. Methodological considerations for the use of stable isotope probing in microbial ecology. *Microb. Ecol.* **2007**, *53*, 435–442. [[CrossRef](#)] [[PubMed](#)]
91. Rajala, P.; Bomberg, M.; Kietäväinen, R.; Kukkonen, I.; Ahonen, L.; Nyysönen, M.; Itävaara, M. Rapid Reactivation of Deep Subsurface Microbes in the Presence of C-1 Compounds. *Microorganisms* **2015**, *3*, 17–33. [[CrossRef](#)] [[PubMed](#)]

